

Two-Stage Context-Aware model for Predicting Future Motion of Dynamic Agents

Sehwan Choi¹Jungho Kim¹Junyong Yun¹Jun Won Choi^{1,2*}¹Hanyang University and ²Qualcomm

{sehwanchoi, jhkim, jyyun}@spa.hanyang.ac.kr

junwchoi@hanyang.ac.kr

Abstract

Predicting the future motion of dynamic agents is of paramount importance to ensure safety or assess risks in motion planning for autonomous robots. In this paper, we propose a two-stage motion prediction method, referred to as R-Pred, that effectively utilizes both the scene and interaction context using a cascade of the initial trajectory proposal network and the trajectory refinement network. The initial trajectory proposal network produces M trajectory proposals corresponding to M modes of a future trajectory distribution. The trajectory refinement network enhances each of M proposals using 1) the tube-query scene attention (TQSA) and 2) the proposal-level interaction attention (PIA). TQSA uses tube-queries to aggregate the local scene context features pooled from proximity around the trajectory proposals of interest. PIA further enhances the trajectory proposals by modeling inter-agent interactions using a group of trajectory proposals selected based on their distances from neighboring agents. Our experiments conducted on the Argoverse and nuScenes datasets demonstrate that the proposed refinement network provides significant performance improvements compared to the single-stage baseline and that R-Pred achieves state-of-the-art performance in some categories of the benchmark.

1. Introduction

In autonomous vehicles and robotics applications, dynamic objects move in complex environments while avoiding collisions with other agents. Each dynamic agent plans its motion by predicting the future motion and behavior of other agents around it. Motion prediction refers to the task of predicting the future trajectory of dynamic agents based on their past trajectory history and information regarding the surrounding environment. The task of predicting motion is challenging because the trajectory of an agent is affected by a variety of contextual factors, which must be considered when modeling the motion. In the context of autonomous

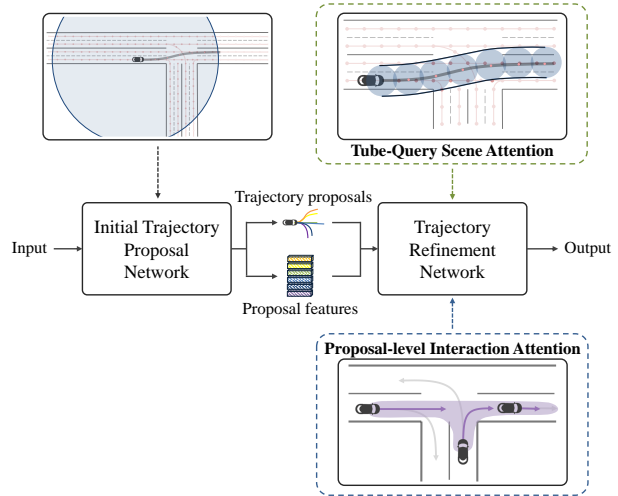


Figure 1. **Key concept of R-Pred.** R-Pred performs two stages of trajectory prediction. ITPNet produces M trajectory proposals with the corresponding proposal features and TRNet refines each trajectory proposals using the separate networks. ITPNet uses a scene context acquired from a relatively large area, whereas TRNet uses a local scene context that exists in a tube-shaped area. TRNet also refines the trajectory proposal using an inter-agent interaction context represented in a proposal level.

vehicles, examples of such factors are provided by permissible road, lane, traffic signals, blinker states, interactions with other agents, and so on. The difficulty in predicting future motion also arises from the fact that the distribution of future trajectories tends to be multi-modal. For a particular scene, a target agent can choose one of the distinct maneuvers (e.g. changing lanes, turning left, turning right or going straight). Accordingly, the prediction model should be able to generate one or more plausible future trajectories with probabilities.

Recently, deep neural networks have opened up a new paradigm in trajectory prediction, achieving considerable performance improvements over traditional prediction models through data-driven modeling of trajectory data.

Sequence modeling architectures such as *long short term memory* (LSTM) [23] or *gated recurrent unit* (GRU) [6] have shown to be effective in representing sequential trajectory data [25, 26], and trajectory prediction task has been successfully performed through encoder-decoder structures [8, 10, 15–17, 19, 20, 24, 26, 28–30, 32, 35, 36, 40, 43, 45, 51, 53]. The accuracy of trajectory prediction can be enhanced by utilizing the various sources of contextual information available for prediction. Numerous methods have jointly modeled the trajectories of multiple neighboring agents to account for their interactions, including social-LSTM [1], soft hardwired attention [12], social GAN [20], MATF [52], Trajectron [24, 40], Desire [28], DATF [36], and Sophie [39]. Static scene information around the target agent can also provide useful clues that can be used to generate more plausible trajectories that conform to the scene’s physical structure. A representation of a scene was obtained by applying a *convolutional neural network* (CNN) to a two-dimensional raster image that describes the scene [4, 7, 11, 32, 37, 50]. A vector representation of the scene was also used for scene encoding, where scene components represented as vectors are encoded using sequence modeling architectures [10, 13, 16, 19, 26, 29, 30, 34, 45, 51, 53]. Recently, Transformer models [44] have been used to encode the scene and interaction context using the attention mechanism [30, 33, 34, 45, 48, 53]. Transformer provides a generic architecture for finding the joint representation of trajectories and vectorized scene components.

In this paper, we propose a new two-stage motion prediction framework, referred to as *R-Pred*. As shown in Fig. 1, the proposed R-Pred architecture consists of two-stage networks: the initial trajectory proposal network (ITPNet) and the trajectory refinement network (TRNet). ITPNet produces M *initial trajectory proposals* corresponding to the M modes of the trajectory distribution for the target agent. These initial trajectory proposals are generated using a global scene context that captures almost all available scene components on the map. TRNet refines each of trajectory proposals by applying M separate refinement networks with shared weights to the latent features called *proposal features* that were responsible for generating the M trajectory proposal. Using the *a priori* trajectory information provided by ITPNet, TRNet can utilize the scene and interaction context in more selective and effective ways. Our *per-proposal refinement strategy* is motivated by two-stage object detectors (e.g., faster RCNN [38]), where the initial object proposals are first obtained from the entire CNN features and then local features in the region of interest (RoI) are pooled to refine each object proposal [18, 21, 38].

TRNet employs the following two refinement sub-modules. First, we devise a *tube-query scene attention* (TQSA) to effectively utilize the scene context. TQSA generates local scene context features obtained within a tube-

shaped area around each trajectory proposal on the map. (see Fig. 1 for illustration.) By doing so, TQSA can only bring in important scene context related to a particular trajectory proposal to cross-attention. Second, we propose the *proposal-level interaction attention* (PIA). PIA models inter-agent interactions using the M trajectory proposals of multiple neighboring agents. PIA employs the *distance-wise grouping strategy*, which selects a group of trajectory proposals that have the greatest influence on each other. For a given trajectory proposal, the proposal with the closest distance is selected from the M trajectory proposals of each neighboring agent. The proposal features corresponding to this proposal group are used to refine the trajectory through cross-attention.

Putting above two refinement methods together, R-Pred can generate refined trajectory outputs. The experiments conducted on widely used Argoverse [5] and nuScenes [3] datasets demonstrate that the proposed refinement network significantly improves the accuracy of the single-stage network baseline. The experiments also show that R-Pred outperforms the latest motion prediction methods and achieves the-state-of-the-art performance in some categories of official Argoverse and nuScenes leaderboards.

The main contributions of our study are summarized below.

- We propose a novel trajectory refinement network that separately refines each of M trajectory proposals using the scene context customized for the trajectory proposal and the proposal-level inter-agent interactions. Our per-proposal refinement strategy can effectively improve the performance of the first-stage network.
- We introduce the concept of global-to-local hierarchical attention to effectively utilize the scene context. While the first-stage network acquires the scene context from a relatively large area around the current location of the target agent, the second-stage network uses tube-queries to gather the scene context from the local area around the proposal trajectory. This strategy allows only important scene information to be used while approaching a solution for trajectory prediction across multiple steps. Proposed global-local hierarchical attention is contrasted with *factorized attention* [33, 34], which iterates attention over different sources of context.
- We use trajectory proposals of neighboring agents to model interactions between agents. Since trajectory proposals capture the particular intention of the agents, the inter-agent interactions can be well modeled using the proposal features. We also propose a simple criterion to group the most influential trajectory proposals for interaction modeling.

- R-Pred can use any *off-the-shelf* single-stage trajectory prediction network as the initial trajectory proposal network. The proposed refinement framework can be readily applied to any single-stage prediction network.
- The source codes used in this study will be released publicly.

2. Related Works

2.1. Context-Aware Trajectory Prediction

Numerous methods have improved the performance of trajectory prediction by leveraging the contextual information available during prediction. Information about the static scene around the target agent was utilized as useful scene context. Raster-based scene encoding summarized scene information using a 2D raster image and extracted the semantic features using convolutional neural networks [4, 9, 14, 32, 37, 40, 46]. The advantage of this approach is that different types of scene components can be easily accommodated in raster images. However, these methods have limited performance due to quantization errors and lack of receptive fields in the encoding architectures. Vector-based scene encoding represented scene components using vectors and encoded their relationship using a graph structure or attention models [10, 13, 20, 24, 27, 29, 40]. VectorNet [13] introduced a hierarchical graph neural network that exploited the spatial locality of road components by vectorized representation. LaneGCN [29] proposed an effective graph convolutional network to represent the complicated topology and long-range dependency. Trajectron++ [40] employed a directed spatio-temporal graph to represent scene context vectors while incorporating agent dynamics and heterogeneous data.

The performance of trajectory prediction has also been improved by taking into account interactions with surrounding dynamic agents and static environment information. Social pooling methods pooled the trajectory features of other agents for interaction modeling [1, 8, 20, 28, 39]. Recently, attention mechanisms have been proposed to exploit the meaningful relationships of dynamic agents and lane segments [10, 13, 16, 19, 26, 29, 29, 32, 41, 45, 49, 53].

2.2. Transformer-based Trajectory Prediction

Transformer provides an efficient architecture for enabling attention mechanism that can capture long-distance dependencies of sequence data. Recently, Transformers have been adopted for trajectory prediction to model context in spatial and temporal domains as well as interactions between agents and maps [30, 33, 34, 45, 48, 53]. mmTransformer [30] employed an efficient stacked Transformer that applied cross-attention on multi-agent context and map context one by one. HiVT [53] summarized

the spatial-temporal features of agents using translation-invariant agent-centric local scene structure. In Scene-Transformer [34], a simple varying form of self-attention for Transformer is exploited to integrate various features, generating scene-level consistent predictions for all agents jointly. Wayformer [33] proposed a general multi-dimensional attention architecture that can jointly encode multiple agent trajectories and map data in time, space, and agent dimensions.

3. Problem Setup

Suppose that the historical trajectory states of the N dynamic agent come from the multi-object tracker, where N can vary depending on a scenario. The agent whose future trajectory is to be predicted is referred to as the target agent and the remaining agents as neighbor agents. The past trajectory states over T time steps for the i -th agent are given by $\mathbf{x}_i = [x_i(t-T+1), x_i(t-T+2), \dots, x_i(t)]$, where t denotes the current time step and $x_i(t-s)$ is the state of the i -th agent at the time step $(t-s)$. The trajectory state is of the form (x, y, ε) consisting of the (x, y) position and the agent’s semantic property ε . The (x, y) coordinates are represented in the agent-centric reference frame, where the current position of a target agent is the origin and its heading angle is aligned with the positive x-axis. Without loss of generality, we let \mathbf{x}_1 be the trajectory of the target agent and $\mathbf{x}_2, \dots, \mathbf{x}_N$ be the trajectories of the neighboring agents. Similarly, the future trajectory states over F time steps for the i -th agent are given by $\mathbf{y}_i = [y_i(t+1), y_i(t+2), \dots, y_i(t+F)]$. We assume that the vector representation of a scene is available along with the trajectory data. For instance, a lane is represented by a set of points on its centerline, where the (x, y) coordinate of each point is expressed in the agent-centric frame. We accommodate different types of scene components by appending an attribute index ϵ_l to the (x, y) coordinate as (x, y, ϵ_l) . The set of scene components around the target agent at the time t is expressed as the vector $\xi = [\xi_1, \dots, \xi_L]$, where the dimension L changes depending on the scene complexity and the region of interest on the map.

Finally, the goal of the motion prediction task is to estimate the future trajectory of the target agent \mathbf{y}_1 given the past trajectories $\mathbf{x}_1, \dots, \mathbf{x}_N$ of N agents and the scene information ξ .

4. Proposed Trajectory Prediction Network

In this section, we present the details of the proposed motion prediction method, R-Pred.

4.1. Overall Framework

An overview of our R-Pred framework is presented in Fig. 2. Our proposed architecture predicts the future tra-

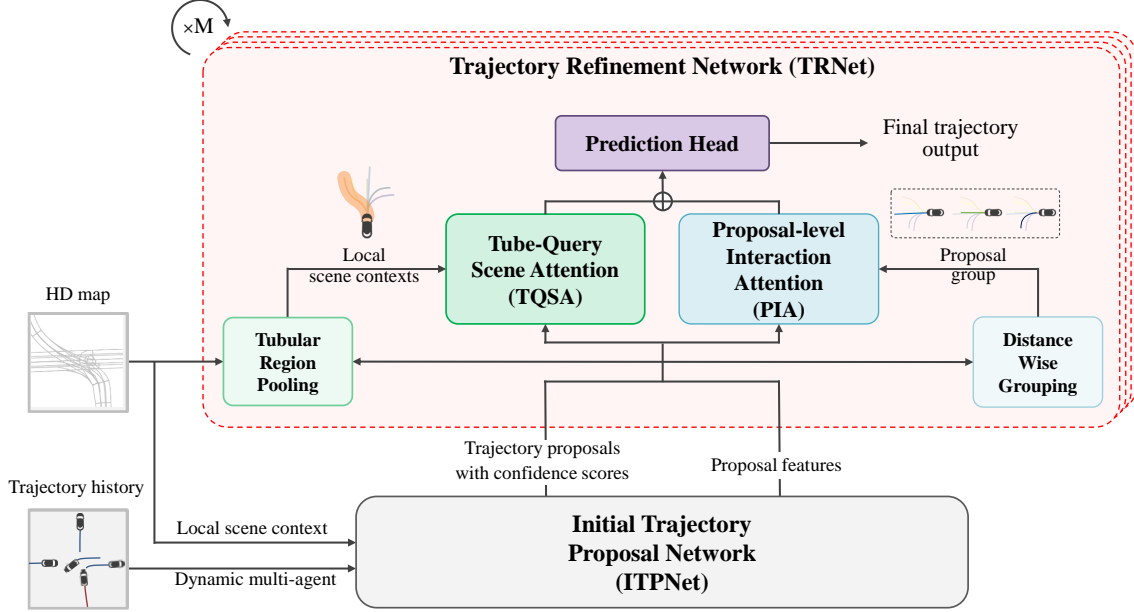


Figure 2. **Overall structure of R-Pred:** Given the past trajectories of the dynamic agents and the scene information, ITPNet generates M trajectory proposals for each agent. TRNet refines each of the M trajectory proposals of the target agent through TQSA and PIA. TQSA utilizes local scene context features obtained by tubular region pooling. PIA captures interaction context using the proposal group found by the *distance-wise proposal grouping*. Finally, the prediction header produces the refined future trajectories based on the joint trajectory features obtained by concatenation of the attention values from TQSA and PIA.

jectory of the target agent over two stages. First, ITPNet produces M trajectory proposals for N agents present in the scene. ITPNet follows traditional methods for scene encoding and interaction encoding. That is, it utilizes the global scene context features extracted from the fixed region around the current position of the agent. Also, ITPNet exploits the interaction context derived from the trajectories of the N agents. TRNet refines each of the M trajectory proposals of the target agent using the initial trajectory information generated by ITPNet. TRNet employs TQSA and PIA to utilize the context for improving the trajectory proposals. First, TQSA extracts local scene context features from a tube-shaped region around the trajectory proposal of the target agent on the map. TQSA enhances the proposal features of the target agent by adaptively aggregating the local scene context features through cross-attention. Second, PIA models inter-agent interaction context using a group of selected proposal trajectories of N agents. *Distance-wise proposal grouping* finds a group of the most influential trajectory proposals between N agents. PIA refines the proposal features of the target agent by aggregating the proposal features of the neighboring agents in the proposal group. The final joint trajectory features are obtained by concatenating two attention values generated by the TQSA and PIA. Based on these features, M future trajectory predictions and their confidence scores are obtained by the *prediction head*.

4.2. Initial Trajectory Proposal Network

ITPNet takes the past trajectories $\mathbf{x}_1, \dots, \mathbf{x}_N$ of the N agents present in the scene and the scene information ξ as input and produces the M trajectory proposals for each agent. For each agent designated as a target agent, ITPNet performs scene encoding and interaction encoding to create joint trajectory features for the target agent. Then, multi-modal prediction head is applied to predict M trajectory proposals and their confidence scores for the target agent, which are returned to the subsequent refinement network. ITPNet also returns the M intermediate features of the prediction head, called *proposal features*, responsible to generate the trajectory proposals. The trajectory proposals, proposal confidence scores, and proposal features for the i -th agent are denoted as $\hat{\mathbf{y}}_i = [\hat{\mathbf{y}}_i^1, \dots, \hat{\mathbf{y}}_i^M]$, $\hat{\mathbf{c}}_i = [\hat{c}_i^1, \dots, \hat{c}_i^M]$, and $\mathbf{f}_i = [\mathbf{f}_i^1, \dots, \mathbf{f}_i^M]$, respectively.

4.3. Trajectory Refinement Network

TRNet refines the trajectory proposals $\hat{\mathbf{y}}_1$ of the target agent using the trajectory proposals $\hat{\mathbf{y}}_1, \dots, \hat{\mathbf{y}}_N$, proposal confidence scores $\hat{\mathbf{c}}_1, \dots, \hat{\mathbf{c}}_N$, proposal features $\mathbf{f}_1, \dots, \mathbf{f}_N$, and the scene information ξ obtained from ITPNet.

Tube-Query Scene Attention. We construct the set of scene embedding features $\Psi = \{\psi_1, \dots, \psi_L\}$ by encoding each element of ξ via a linear projection, i.e., $\psi_l = \text{linear_proj}(\xi_l)$. TQSA pools the scene embedding features

Algorithm 1 Tubular Region Pooling

Input: Trajectory proposal \hat{y}_1^m , scene context vectors ξ , scene embedding features Ψ , and thresholding radius τ .

Output: Local scene context features Ψ_1^m .

- 1: $\Psi_1^m = \text{set}()$
- 2: **for** $f \leftarrow t + 1$ to $t + F$ **do**
- 3: **for** each $\xi_l \in \xi$ **do**
- 4: $dist = \|(\hat{y}_1^m(f) - \xi_l)\|_2^2$
- 5: **if** $dist < \tau$ **then**
- 6: $\Psi_1^m.\text{add}(\psi_l)$
- 7: **end if**
- 8: **end for**
- 9: **end for**
- 10: **return** Ψ_1^m

in a tubular region around the trajectory proposal on the map from Ψ . We denote the set of scene embedding features pooled for the trajectory proposal \hat{y}_1^m of the target agent as Ψ_1^m . *Tubular region pooling* is efficiently performed by aggregating scene embedding features within the search radius τ around each waypoint of the trajectory proposal. Note that a collection of search disks centered at all waypoints on the trajectory forms an approximately tubular polygon. See the Algorithm 1 for details.

TQSA decodes the proposal features \mathbf{f}_1^m of the target agent by performing cross-attention on the local scene context Ψ_1^m . Specifically, we use the proposal features \mathbf{f}_1^m as query and the local scene context features Ψ_1^m as key and value, i.e.,

$$Q = \mathbf{f}_1^m W^{Q_{TQSA}} \quad (1)$$

$$K = \Psi_1^m W^{K_{TQSA}} \quad (2)$$

$$V = \Psi_1^m W^{V_{TQSA}} \quad (3)$$

$$\mathcal{A}_1^m = \text{softmax} \left(\frac{QK^\top}{\sqrt{d_k}} \right) V, \quad (4)$$

where $W^{Q_{TQSA}}$, $W^{K_{TQSA}}$, and $W^{V_{TQSA}}$ are learnable weight matrices and d_k is the dimension of embedding vectors. We combine the attention value \mathcal{A}_1^m and the proposal features \mathbf{f}_1 using the gating function introduced in [53]

$$\lambda = \sigma(\mathbf{f}_1^m W^{input} + \mathcal{A}_1^m W^{hidden}) \quad (5)$$

$$\mathbf{t}_1^m = \lambda \odot \mathbf{f}_1^m W^{gate} + (1 - \lambda) \odot \mathcal{A}_1^m \quad (6)$$

$$\mathbf{t}_1^m = \mathbf{f}_1^m + \phi(\mathbf{t}_1^m), \quad (7)$$

where W^{input} , W^{hidden} , and W^{gate} are learnable matrices, \odot indicates element-wise product, σ indicates the sigmoid function and $\phi(\cdot)$ denotes a *multi-layer perceptron* (MLP). We add *layer normalization* [2], *Dropout* [42], and *residual connection* [22] in the middle of the attention process.

Algorithm 2 Distance-Wise Grouping Algorithm

Input: Trajectory proposals $\hat{y}_1, \dots, \hat{y}_N$, proposal confidence scores $\hat{c}_1, \dots, \hat{c}_N$, proposal features $\mathbf{f}_1, \dots, \mathbf{f}_N$, and confidence threshold T .

Output: Proposal group set $\mathcal{G}(\hat{y}_1^m)$.

- 1: $\mathcal{G}(\hat{y}_1^m) = \{\}$
- 2: **for** $i \leftarrow 2$ to N **do**
- 3: $\mathcal{B} = \{\}$
- 4: **for** $m' \leftarrow 1$ to M **do**
- 5: **if** $\hat{c}_i^{m'} > T$ **then**
- 6: $\mathcal{B}.\text{append}(m')$
- 7: **end if**
- 8: **end for**
- 9: $m_i = \underset{l \in \mathcal{B}}{\text{argmin}} \sum_{f=t+1}^{t+F} \|(\hat{y}_1^m(f) - \hat{y}_i^l(f))\|_2^2$
- 10: $\mathcal{G}(\hat{y}_1^m).\text{append}(\mathbf{f}_i^{m_i})$
- 11: **end for**
- 12: **return** $\mathcal{G}(\hat{y}_1^m)$

Note that the aforementioned local scene attention process to produce the output of TQSA \mathbf{t}_1^m is performed for each trajectory proposal (for each m value) in parallel.

Proposal-level Interaction Attention. PIA uses the *distance-wise proposal grouping* algorithm to find a group of the trajectory proposals for N agents for interaction modeling. First, among MN trajectory proposals from N agents, the trajectory proposals with a confidence score below the threshold T are discarded as they are unlikely to occur. Then, for a given trajectory proposal \hat{y}_1^m of the target agent, the algorithm chooses the closest one among the M trajectory proposals of each neighboring agent. The algorithm returns a proposal group $\{\hat{y}_2^{m_2}, \dots, \hat{y}_N^{m_N}\}$, where m_2, \dots, m_N are the indices of the selected trajectory proposals. The *distance-wise proposal grouping* algorithm is summarized in Algorithm 2.

The set of proposal features in the proposal group is given by

$$\mathcal{G}(\hat{y}_1^m) = \{\mathbf{f}_2^{m_2}, \dots, \mathbf{f}_N^{m_N}\}, \quad (8)$$

and used to decode the proposal features \mathbf{f}_1^m through cross-attention. Using \mathbf{f}_1^m as query and $\mathcal{G}(\mathbf{f}_1^m)$ as key and value, the cross-attention module produces the attention value \mathbf{p}_1^m in a similar way to (1) - (7).

Multi-modal Prediction Head. TRNet generates the final joint trajectory features \mathbf{j}_1^m for the target agent by concatenating the output of TQSA \mathbf{t}_1^m and the output of PIA \mathbf{p}_1^m . Then, the prediction head produces the refined trajectory output based on the joint trajectory features. The prediction head consists of the regression branch and classification branch. Modeling the trajectory points as multivariate random vectors with independent Laplace distribution, the regression branch applies MLP to predict the mean

Method	minADE ₁	minFDE ₁	minADE ₆	minFDE ₆	brierFDE ₆	MR ₆ %
LaneRCNN [49]	1.69	3.69	0.90	1.45	2.15	12.3
LaPred [26]	1.93	4.33	0.91	1.50	2.13	18.0
TNT [51]	2.17	4.96	0.91	1.45	2.14	16.6
PRIME [41]	1.91	3.82	1.22	1.56	2.10	11.5
HOME [14]	1.72	3.73	0.92	1.36	-	11.3
LaneGCN [29]	1.70	3.76	0.87	1.36	2.05	16.2
mmTransformer [30]	1.77	4.00	0.84	1.34	2.03	15.4
DenseTNT [19]	1.68	3.63	0.88	1.28	1.98	12.6
THOMAS [16]	1.67	3.59	0.94	1.44	1.97	10.3
SceneTransformer [34]	1.81	3.62	0.80	1.23	1.89	12.5
LTP [45]	1.62	3.55	0.83	1.30	1.86	14.7
HOME+GOHOME [15]	1.70	3.68	0.89	1.29	1.86	8.5
TPCN [47]	1.66	3.69	0.87	1.38	-	15.8
MultiPath++ [43]	1.62	3.61	0.79	1.21	1.79	13.2
Wayformer [33]	1.64	3.67	0.77	1.16	1.74	11.9
HiVT(Singe-stage baseline) [53]	1.60	3.52	0.77	1.17	1.84	12.7
Ours	1.59	3.50	0.76	1.13	1.79	11.6

Table 1. Performance comparison on *Argoverse test set*. The best performed metrics are bolded. The “-” symbol means the corresponding metric unknown, because the author have not disclosed it or it is not specified in the leaderboard. Our model achieves the state-of-the-art performance in *minADE₁*, *minFDE₁*, *minADE₆* and *minFDE₆* metrics.

and covariance of \mathbf{y}_1^m . The predicted mean is denoted as $\check{\mathbf{y}}_1^m = [\check{y}_1^m(t+1), \dots, \check{y}_1^m(t+F)]$ and the predicted variance is denoted as $\check{\mathbf{b}}_1^m = [\check{b}_1^m(t+1), \dots, \check{b}_1^m(t+F)]$. The classification branch applies another MLP to produce the confidence scores for M modes, $\check{\mathbf{c}}_1 = [\check{c}_1^1, \dots, \check{c}_1^M]$.

4.4. Training Details

ITPNet and TRNet of R-Pred can be jointly trained end-to-end. The total loss function L_{total} used to train the entire network is given by

$$L_{total} = \alpha L_{reg_pro} + \beta L_{cls_pro} + \gamma L_{reg_ref} + \delta L_{cls_ref},$$

where L_{reg_pro} and L_{reg_ref} are the regression loss functions for ITPNet, and TRNet and L_{cls_pro} and L_{cls_ref} are the classification loss functions for ITPNet, and TRNet. We used $\alpha = \beta = \gamma = \delta = 1$ in our setup. Negative log-likelihood function for Laplace distribution is used for L_{reg_ref}

$$L_{reg_ref} = -\frac{1}{NF} \sum_{n=1}^N \sum_{f=t+1}^{t+F} \frac{1}{2\check{b}_n^m(f)} e^{-\frac{|y_n(f) - \check{y}_n^m(f)|}{\check{b}_n^m(f)}}.$$

L_{reg_pro} is defined similarly. When we evaluate the loss function during training, we adopt *winner-takes-all* strategy [7] that uses the mode m^* of the trajectory output that yields the smallest final displacement error, i.e., $m^* = \operatorname{argmin}_m |y_n(t+F) - \check{y}_n^m(t+F)|$. We use the cross entropy loss for L_{cls_pro} and L_{cls_ref} .

5. Experiments

In this section, we evaluate the performance of the proposed R-Pred and provide both quantitative and qualitative analysis on the behavior of the model.

Datasets. Both Argoverse [5] and nuScenes [3] datasets provide dynamic agent trajectories and HD-map in real-world driving scenarios. Argoverse dataset was collected in two US cities, Miami and Pittsburgh. Each sample contains 5 second trajectories of tracked vehicles sampled at 10 hertz. Argoverse dataset provides HD-map with detailed lane information. The prediction task is to predict future trajectories for 3 seconds given past trajectories of 2 seconds. The dataset contains 205,942 training, 39,272 validation, and 78,143 test samples.

nuScenes dataset is collected in Boston and Singapore. The trajectories collected are 6-seconds long and sampled at 2 hertz. The prediction task is to predict future trajectories for 6 seconds given past trajectories of 2 seconds. HD-map is also provided with the trajectory data. The dataset is split into 32,186 training, 8,560 validation, and 9,041 test samples.

Metrics. For performance evaluation, we adopt the widely used performance metrics including *average displacement error (ADE)*, *final displacement error (FDE)*, and *miss rate (MR)*. *ADE* refers to the mean square error with the ground truth over the entire time steps, and *FDE* is defined as the average displacement error at the endpoint. We evaluate the prediction accuracy with $M > 1$ trajectory

Method	$minADE_1$	$minFDE_1$	$minADE_5$	$minFDE_5$	$minADE_{10}$	$minFDE_{10}$
MTP [7]	4.42	10.36	2.22	4.83	1.74	3.54
CoverNet [37]	3.87	9.26	1.96	-	1.48	-
Trajectron++ [40]	-	9.52	1.88	-	1.51	-
MHA-JAM [32]	3.69	8.57	1.81	3.72	1.24	2.21
MultiPath [4]	4.43	10.16	1.78	3.62	1.55	2.93
CXX [31]	-	-	1.63	-	1.29	-
LaPred [26]	3.51	8.12	1.53	3.37	1.12	2.39
P2T [9]	-	-	1.45	-	1.16	-
THOMAS [16]	-	-	1.33	-	1.04	-
PGP(Singe-stage baseline) [10]	-	7.34	1.30	-	0.98	-
Ours	3.34	7.74	1.19	2.28	0.95	1.59

Table 2. Performance comparison on *nuScenes validation set*. The “-” symbol means the corresponding metric unknown. Our model achieves the state-of-the-art performance on all metrics.

Single-stage	TQSA	PIA	Refinement input format	Local scene pooling	$minADE_6$	$minFDE_6$	$MR_6\%$
✓	✓	✓	✓	✓	0.644	0.914	8.49
✓		✓	✓		$0.658_{\downarrow 2.17\%}$	$0.962_{\downarrow 5.25\%}$	$9.17_{\downarrow 8.01\%}$
✓	✓		✓	✓	$0.648_{\downarrow 0.62\%}$	$0.926_{\downarrow 1.31\%}$	$8.91_{\downarrow 4.95\%}$
✓	✓	✓		✓	$0.654_{\downarrow 1.55\%}$	$0.950_{\downarrow 3.94\%}$	$9.07_{\downarrow 6.83\%}$
✓	✓	✓	✓		$0.649_{\downarrow 0.78\%}$	$0.926_{\downarrow 1.31\%}$	$8.89_{\downarrow 4.71\%}$
✓					$0.686_{\downarrow 6.52\%}$	$1.040_{\downarrow 13.79\%}$	$10.2_{\downarrow 20.14\%}$

Table 3. Ablation study conducted on *Argoverse validation set*. *Refinement input format* denotes that proposal features are used as input of TRNet on behalf of trajectory proposals. The *Local scene pooling* indicates that the local scene context generated by tubular region pooling is exploited as input of TQSA.

predictions using $minADE_M$ and $minFDE_M$, which are minimum ADE and FDE over M predicted trajectories. MR_M measures the ratio within 2 meters between the endpoint of the best-predicted trajectory and ground truth. We also use *brier minimum FDE* ($brierFDE_M$), which measures the value of $minFDE_M + (1 - p)^2$, where p is the highest confidence score among M trajectories. It imposes a penalty when the probability of the best trajectory is low. **Implementation Details.** We set the threshold τ of TQSA to 20 meter and T of PIA to 0.1. The embedding size of all features was set to 128 for comparative performance analysis. The embedding size was to 64 for the ablation study to shorten the training time. We used the existing prediction architectures as ITPNet. We chose HiVT [53] on Argoverse and PGP [10] on nuScenes for ITPNet. These models achieved excellent performance in both benchmarks respectively. They are considered as singe-stage baselines used to measure the performance gain achieved by our refinement network. We trained our model on TiTAN RTX for 64 epochs with 32 batch sizes. The data was batched randomly. For all experiments, we trained the model using AdamW optimizer with an initial learning rate of 5e-4. The learning

rate decays using cosine annealing. We used dropout with a 0.1 ratio. Data augmentation was not used. A more detailed setup is provided in Supplementary Material.

5.1. Quantitative Results

Table 1 presents the performance of R-Pred evaluated on *Argoverse test set*. We compare R-Pred with several top ranked models [14–16, 19, 29, 30, 33, 34, 41, 43, 45, 47, 49, 51]. Pred achieves the best prediction accuracy in $minADE_1$, $minFDE_1$, $minADE_6$ and $minFDE_6$ metrics and competitive performance in $brierFDE_6$ and MR_6 . R-Pred sets a new state-of-the-art performance surpassing the current best methods, Wayformer [33] and MultiPath++ [43]. Compared to the single-stage HiVT baseline [53], the proposed method offers performance improvements of 1.29% and 3.41% in $minADE_6$, and $minFDE_6$, respectively. This indicates that our trajectory refinement strategy can effectively improve the reliability and robustness of the initial prediction by ITPNet.

Table 2 presents the performance of several motion prediction methods on *nuScenes validation set*. We compare R-Pred with the top rankers [4, 9, 10, 16, 26, 31, 32, 37, 40]

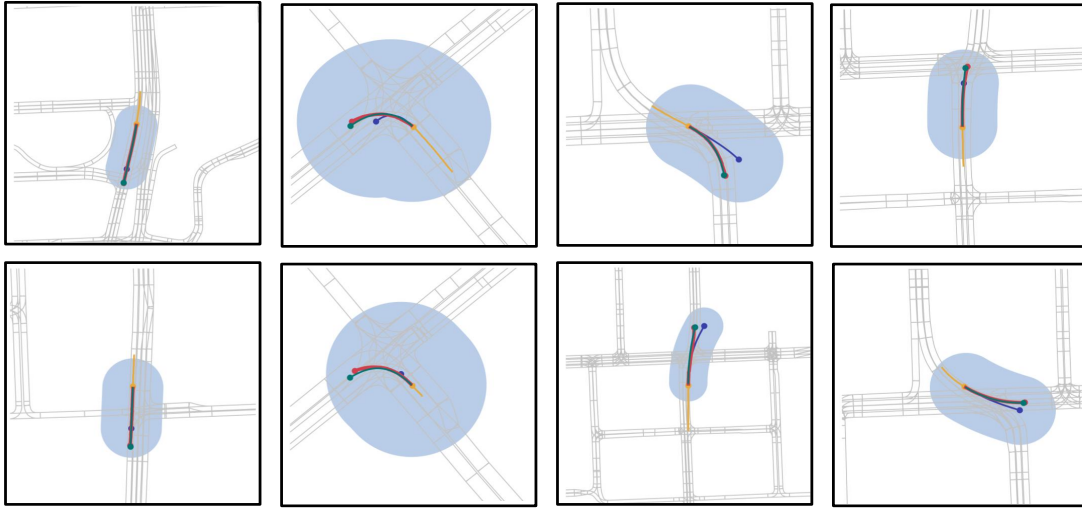


Figure 3. Qualitative results of R-Pred on *Argoverse validation set*. Yellow, red, blue, and green lines represent the history, ground truth, the initial proposal with the highest score, and the final (refined) trajectory, respectively. The sky blue region denotes tubular regions used for TQSA. These figures present different vehicle motion scenarios such as going straight, turning left, slowing down, changing lanes, etc.

in nuScenes leaderboard. R-Pred achieves significant performance gains over the other prediction methods. R-Pred offers 8.46% and 3.06% reductions in $minADE_5$ and $minADE_{10}$ compared to single-stage PGP baseline [10].

5.2. Ablation Study

Table 3 presents the ablation study that reveals the contributions of each component to overall performance achieved by R-Pred. Our evaluation is performed on *Argoverse validation set*. We investigate how much performance degrades as each component is removed from R-Pred. We consider the following four components of R-Pred: 1) TQSA, 2) PIA, 3) refinement input format, and 4) local scene pooling. When TQSA is disabled, $minFDE_6$ drops by 5.25%, which shows that TQSA plays a significant role in improving performance. Disabling PIA results in a 1.31% performance loss in $minFDE_6$. We attempt to change the input format of TRNet from the proposal features to the trajectory proposals. In this case, the trajectory proposals should be re-encoded for refinement. We confirm the benefit of using the proposal features for the refinement network in the ablation study. We also attempt to use global scene features rather than local scene features for cross-attention in TQSA. When the global scene features are used, the performance in $minFDE_6$ drops by 1.31%. Finally, the combination of all these components provides a 13.79% performance improvement over a single-stage baseline.

5.3. Qualitative Results

Fig. 3 shows a visualization of the actual predicted trajectory samples generated by R-Pred using *Argoverse val-*

idation set. We visualize the final trajectory with the best score produced by R-Pred (green line) and the corresponding trajectory proposal from ITPNet (blue line). We also include the ground truth trajectory (red line). We added the tubular area used for TQSA to the figure. We observe that our refinement network reduces the prediction error in the trajectories generated by ITPNet. Note that in third column, our refinement stage modifies the initial trajectory proposal off-road to the trajectory within the road. More qualitative results are provided in Supplementary Material.

6. Conclusions

In this paper, we proposed a two-stage trajectory prediction method, referred to as R-Pred. We introduced a novel *per proposal trajectory refinement* strategy in which each trajectory proposal generated in the first-stage network is refined using contextual information tailored to the proposal. TRNet utilized the local scene context captured by pooling scene component features in a tubular region around the trajectory proposal. TRNet also used the inter-agent interaction context inferred from a group of the most influential trajectory proposals of neighboring agents. Our evaluation conducted on Argoverse and nuScenes benchmarks confirmed that R-Pred significantly outperformed the existing methods and achieved the-state-of-the-art performance in some evaluation metrics.

References

- [1] Alexandre Alahi, Kratarth Goel, Vignesh Ramanathan, Alexandre Robicquet, Li Fei-Fei, and Silvio Savarese. Social lstm: Human trajectory prediction in crowded spaces. In

In Proceedings of the IEEE conference on computer vision and pattern recognition (CVPR), pages 961–971, 2016. 2, 3

[2] Jimmy Lei Ba, Jamie Ryan Kiros, and Geoffrey E Hinton. Layer normalization. *arXiv preprint arXiv:1607.06450*, 2016. 5

[3] Holger Caesar, Varun Bankiti, Alex H Lang, Sourabh Vora, Venice Erin Liong, Qiang Xu, Anush Krishnan, Yu Pan, Giacarlo Baldan, and Oscar Beijbom. nuscenes: A multimodal dataset for autonomous driving. In *In Proceedings of the IEEE/CVF conference on computer vision and pattern recognition (CVPR)*, pages 11621–11631, 2020. 2, 6

[4] Yuning Chai, Benjamin Sapp, Mayank Bansal, and Dragomir Anguelov. Multipath: Multiple probabilistic anchor trajectory hypotheses for behavior prediction. In *In Conference on Robot Learning (CoRL)*, pages 86–99, 2020. 2, 3, 7

[5] Ming-Fang Chang, John Lambert, Patsorn Sangkloy, Jagjeet Singh, Slawomir Bak, Andrew Hartnett, De Wang, Peter Carr, Simon Lucey, Deva Ramanan, et al. Argoverse: 3d tracking and forecasting with rich maps. In *In Proceedings of the IEEE/CVF Conference on Computer Vision and Pattern Recognition (CVPR)*, pages 8748–8757, 2019. 2, 6

[6] Junyoung Chung, Caglar Gulcehre, KyungHyun Cho, and Yoshua Bengio. Empirical evaluation of gated recurrent neural networks on sequence modeling. *arXiv preprint arXiv:1412.3555*, 2014. 2

[7] Henggang Cui, Vladan Radosavljevic, Fang-Chieh Chou, Tsung-Han Lin, Thi Nguyen, Tzu-Kuo Huang, Jeff Schneider, and Nemanja Djuric. Multimodal trajectory predictions for autonomous driving using deep convolutional networks. In *In 2019 International Conference on Robotics and Automation (ICRA)*, pages 2090–2096, 2019. 2, 6, 7

[8] Nachiket Deo and Mohan M Trivedi. Convolutional social pooling for vehicle trajectory prediction. In *In Proceedings of the IEEE Conference on Computer Vision and Pattern Recognition Workshops (CVPRW)*, pages 1468–1476, 2018. 2, 3

[9] Nachiket Deo and Mohan M Trivedi. Trajectory forecasts in unknown environments conditioned on grid-based plans. *arXiv preprint arXiv:2001.00735*, 2020. 3, 7

[10] Nachiket Deo, Eric Wolff, and Oscar Beijbom. Multimodal trajectory prediction conditioned on lane-graph traversals. In *In Conference on Robot Learning (CoRL)*, pages 203–212, 2022. 2, 3, 7, 8

[11] Nemanja Djuric, Vladan Radosavljevic, Henggang Cui, Thi Nguyen, Fang-Chieh Chou, Tsung-Han Lin, Nitin Singh, and Jeff Schneider. Uncertainty-aware short-term motion prediction of traffic actors for autonomous driving. In *In Proceedings of the IEEE/CVF Winter Conference on Applications of Computer Vision (WACV)*, pages 2095–2104, 2020. 2

[12] Tharindu Fernando, Simon Denman, Sridha Sridharan, and Clinton Fookes. Soft+ hardwired attention: An lstm framework for human trajectory prediction and abnormal event detection. *Neural networks*, 108:466–478, 2018. 2

[13] Jiyang Gao, Chen Sun, Hang Zhao, Yi Shen, Dragomir Anguelov, Congcong Li, and Cordelia Schmid. Vectornet: Encoding hd maps and agent dynamics from vectorized representation. In *In Proceedings of the IEEE/CVF Conference on Computer Vision and Pattern Recognition (CVPR)*, pages 11525–11533, 2020. 2, 3

[14] Thomas Gilles, Stefano Sabatini, Dzmitry Tsishkou, Bogdan Stanciulescu, and Fabien Moutarde. Home: Heatmap output for future motion estimation. In *In 2021 IEEE International Intelligent Transportation Systems Conference (ITSC)*, pages 500–507, 2021. 3, 6, 7

[15] Thomas Gilles, Stefano Sabatini, Dzmitry Tsishkou, Bogdan Stanciulescu, and Fabien Moutarde. Gohome: Graph-oriented heatmap output for future motion estimation. In *In 2022 International Conference on Robotics and Automation (ICRA)*, pages 9107–9114, 2022. 2, 6, 7

[16] Thomas Gilles, Stefano Sabatini, Dzmitry Tsishkou, Bogdan Stanciulescu, and Fabien Moutarde. Thomas: Trajectory heatmap output with learned multi-agent sampling. In *In International Conference on Learning Representations (ICLR)*, 2022. 2, 3, 6, 7

[17] Roger Girgis, Florian Golemo, Felipe Codevilla, Martin Weiss, Jim Aldon D’Souza, Samira Ebrahimi Kahou, Felix Heide, and Christopher Pal. Latent variable sequential set transformers for joint multi-agent motion prediction. In *In International Conference on Learning Representations (ICLR)*, 2021. 2

[18] Ross Girshick. Fast r-cnn. In *In Proceedings of the IEEE/CVF International Conference on Computer Vision (ICCV)*, pages 1440–1448, 2015. 2

[19] Junru Gu, Chen Sun, and Hang Zhao. Densentnt: End-to-end trajectory prediction from dense goal sets. In *In Proceedings of the IEEE/CVF International Conference on Computer Vision (ICCV)*, pages 15303–15312, 2021. 2, 3, 6, 7

[20] Agrim Gupta, Justin Johnson, Li Fei-Fei, Silvio Savarese, and Alexandre Alahi. Social gan: Socially acceptable trajectories with generative adversarial networks. In *In Proceedings of the IEEE conference on computer vision and pattern recognition (CVPR)*, pages 2255–2264, 2018. 2, 3

[21] Kaiming He, Georgia Gkioxari, Piotr Dollár, and Ross Girshick. Mask r-cnn. In *In Proceedings of the IEEE/CVF International Conference on Computer Vision (ICCV)*, pages 2961–2969, 2017. 2

[22] Kaiming He, Xiangyu Zhang, Shaoqing Ren, and Jian Sun. Deep residual learning for image recognition. In *In Proceedings of the IEEE conference on computer vision and pattern recognition (CVPR)*, pages 770–778, 2016. 5

[23] Sepp Hochreiter and Jürgen Schmidhuber. Long short-term memory. *Neural computation*, 9(8):1735–1780, 1997. 2

[24] Boris Ivanovic and Marco Pavone. The trajectron: Probabilistic multi-agent trajectory modeling with dynamic spatiotemporal graphs. In *In Proceedings of the IEEE/CVF International Conference on Computer Vision (ICCV)*, pages 2375–2384, 2019. 2, 3

[25] ByeoungDo Kim, Chang Mook Kang, Jaekyung Kim, Seung Hi Lee, Chung Choo Chung, and Jun Won Choi. Probabilistic vehicle trajectory prediction over occupancy grid map via recurrent neural network. In *In 2017 IEEE 20th International Conference on Intelligent Transportation Systems (ITSC)*, pages 399–404, 2017. 2

[26] ByeoungDo Kim, Seong Hyeon Park, Seokhwan Lee, Elbek Khoshimjonov, Dongsuk Kum, Junsoo Kim, Jeong Soo Kim,

and Jun Won Choi. Lapred: Lane-aware prediction of multi-modal future trajectories of dynamic agents. In *In Proceedings of the IEEE/CVF Conference on Computer Vision and Pattern Recognition (CVPR)*, pages 14636–14645, 2021. 2, 3, 6, 7

[27] Sumit Kumar, Yiming Gu, Jerrick Hoang, Galen Clark Haynes, and Micol Marchetti-Bowick. Interaction-based trajectory prediction over a hybrid traffic graph. In *In 2021 IEEE/RSJ International Conference on Intelligent Robots and Systems (IROS)*, pages 5530–5535, 2021. 3

[28] Namhoon Lee, Wongun Choi, Paul Vernaza, Christopher B Choy, Philip HS Torr, and Manmohan Chandraker. Desire: Distant future prediction in dynamic scenes with interacting agents. In *In Proceedings of the IEEE conference on computer vision and pattern recognition (CVPR)*, pages 336–345, 2017. 2, 3

[29] Ming Liang, Bin Yang, Rui Hu, Yun Chen, Renjie Liao, Song Feng, and Raquel Urtasun. Learning lane graph representations for motion forecasting. In *In European Conference on Computer Vision (ECCV)*, pages 541–556, 2020. 2, 3, 6, 7

[30] Yicheng Liu, Jinghuai Zhang, Liangji Fang, Qinhong Jiang, and Bolei Zhou. Multimodal motion prediction with stacked transformers. In *In Proceedings of the IEEE/CVF Conference on Computer Vision and Pattern Recognition (CVPR)*, pages 7577–7586, 2021. 2, 3, 6, 7

[31] Chenxu Luo, Lin Sun, Dariush Dabiri, and Alan Yuille. Probabilistic multi-modal trajectory prediction with lane attention for autonomous vehicles. In *In 2020 IEEE/RSJ International Conference on Intelligent Robots and Systems (IROS)*, pages 2370–2376, 2020. 7

[32] Kaouther Messaoud, Nachiket Deo, Mohan M Trivedi, and Fawzi Nashashibi. Trajectory prediction for autonomous driving based on multi-head attention with joint agent-map representation. In *In 2021 IEEE Intelligent Vehicles Symposium (IV)*, pages 165–170, 2021. 2, 3, 7

[33] Nigamaa Nayakanti, Rami Al-Rfou, Aurick Zhou, Kratarth Goel, Khaled S Refaat, and Benjamin Sapp. Wayformer: Motion forecasting via simple & efficient attention networks. *arXiv preprint arXiv:2207.05844*, 2022. 2, 3, 6, 7

[34] Jiquan Ngiam, Vijay Vasudevan, Benjamin Caine, Zhengdong Zhang, Hao-Tien Lewis Chiang, Jeffrey Ling, Rebecca Roelofs, Alex Bewley, Chenxi Liu, Ashish Venugopal, et al. Scene transformer: A unified architecture for predicting future trajectories of multiple agents. In *In International Conference on Learning Representations (ICLR)*, 2022. 2, 3, 6, 7

[35] Seong Hyeon Park, ByeongDo Kim, Chang Mook Kang, Chung Choo Chung, and Jun Won Choi. Sequence-to-sequence prediction of vehicle trajectory via lstm encoder-decoder architecture. In *In 2018 IEEE Intelligent Vehicles Symposium (IV)*, pages 1672–1678, 2018. 2

[36] Seong Hyeon Park, Gyubok Lee, Jimin Seo, Manoj Bhat, Minseok Kang, Jonathan Francis, Ashwin Jadhav, Paul Pu Liang, and Louis-Philippe Morency. Diverse and admissible trajectory forecasting through multimodal context understanding. In *In European Conference on Computer Vision (ECCV)*, pages 282–298, 2020. 2

[37] Tung Phan-Minh, Elena Corina Grigore, Freddy A Boulton, Oscar Beijbom, and Eric M Wolff. Covernet: Multimodal behavior prediction using trajectory sets. In *In Proceedings of the IEEE/CVF Conference on Computer Vision and Pattern Recognition (CVPR)*, pages 14074–14083, 2020. 2, 3, 7

[38] Shaoqing Ren, Kaiming He, Ross Girshick, and Jian Sun. Faster r-cnn: Towards real-time object detection with region proposal networks. *Advances in neural information processing systems*, 28, 2015. 2

[39] Amir Sadeghian, Vineet Kosaraju, Ali Sadeghian, Noriaki Hirose, Hamid Rezatofighi, and Silvio Savarese. Sophie: An attentive gan for predicting paths compliant to social and physical constraints. In *In Proceedings of the IEEE/CVF conference on computer vision and pattern recognition (CVPR)*, pages 1349–1358, 2019. 2, 3

[40] Tim Salzmann, Boris Ivanovic, Punarjay Chakravarty, and Marco Pavone. Trajectron++: Dynamically-feasible trajectory forecasting with heterogeneous data. In *In European Conference on Computer Vision (ECCV)*, pages 683–700, 2020. 2, 3, 7

[41] Haoran Song, Di Luan, Wenchao Ding, Michael Y Wang, and Qifeng Chen. Learning to predict vehicle trajectories with model-based planning. In *Conference on Robot Learning*, pages 1035–1045, 2022. 3, 6, 7

[42] Nitish Srivastava, Geoffrey Hinton, Alex Krizhevsky, Ilya Sutskever, and Ruslan Salakhutdinov. Dropout: a simple way to prevent neural networks from overfitting. *The journal of machine learning research*, 15(1):1929–1958, 2014. 5

[43] Balakrishnan Varadarajan, Ahmed Hefny, Avikalp Srivastava, Khaled S Refaat, Nigamaa Nayakanti, Andre Cornman, Kan Chen, Bertrand Douillard, Chi Pang Lam, Dragomir Anguelov, et al. Multipath++: Efficient information fusion and trajectory aggregation for behavior prediction. In *In 2022 International Conference on Robotics and Automation (ICRA)*, pages 7814–7821, 2022. 2, 6, 7

[44] Ashish Vaswani, Noam Shazeer, Niki Parmar, Jakob Uszkoreit, Llion Jones, Aidan N Gomez, Łukasz Kaiser, and Illia Polosukhin. Attention is all you need. *Advances in neural information processing systems*, 30, 2017. 2

[45] Jingke Wang, Tengju Ye, Ziqing Gu, and Junbo Chen. Ltp: Lane-based trajectory prediction for autonomous driving. In *In Proceedings of the IEEE/CVF Conference on Computer Vision and Pattern Recognition (CVPR)*, pages 17134–17142, 2022. 2, 3, 6, 7

[46] David Wu and Yunnan Wu. air² for interaction prediction. *arXiv preprint arXiv:2111.08184*, 2021. 3

[47] Maosheng Ye, Tongyi Cao, and Qifeng Chen. Tpcn: Temporal point cloud networks for motion forecasting. In *Proceedings of the IEEE/CVF Conference on Computer Vision and Pattern Recognition*, pages 11318–11327, 2021. 6, 7

[48] Ye Yuan, Xinshuo Weng, Yanglan Ou, and Kris M Kitani. Agentformer: Agent-aware transformers for socio-temporal multi-agent forecasting. In *In Proceedings of the IEEE/CVF International Conference on Computer Vision (ICCV)*, pages 9813–9823, 2021. 2, 3

[49] Wenyuan Zeng, Ming Liang, Renjie Liao, and Raquel Urtasun. Lanercnn: Distributed representations for graph-centric

motion forecasting. In *2021 IEEE/RSJ International Conference on Intelligent Robots and Systems (IROS)*, pages 532–539, 2021. [3](#), [6](#), [7](#)

[50] Lingyao Zhang, Po-Hsun Su, Jerrick Hoang, Galen Clark Haynes, and Micol Marchetti-Bowick. Map-adaptive goal-based trajectory prediction. In *In Conference on Robot Learning (CoRL)*, pages 1371–1383, 2021. [2](#)

[51] Hang Zhao, Jiyang Gao, Tian Lan, Chen Sun, Ben Sapp, Balakrishnan Varadarajan, Yue Shen, Yi Shen, Yuning Chai, Cordelia Schmid, et al. Tnt: Target-driven trajectory prediction. In *In Conference on Robot Learning (CoRL)*, pages 895–904, 2021. [2](#), [6](#), [7](#)

[52] Tianyang Zhao, Yifei Xu, Mathew Monfort, Wongun Choi, Chris Baker, Yibiao Zhao, Yizhou Wang, and Ying Nian Wu. Multi-agent tensor fusion for contextual trajectory prediction. In *In Proceedings of the IEEE/CVF Conference on Computer Vision and Pattern Recognition (CVPR)*, pages 12126–12134, 2019. [2](#)

[53] Zikang Zhou, Luyao Ye, Jianping Wang, Kui Wu, and Kejie Lu. Hivt: Hierarchical vector transformer for multi-agent motion prediction. In *In Proceedings of the IEEE/CVF Conference on Computer Vision and Pattern Recognition (CVPR)*, pages 8823–8833, 2022. [2](#), [3](#), [5](#), [6](#), [7](#)

Supplementary Material

A. The Detailed Network Architecture

Fig. 4 presents the detailed network architecture of our R-Pred. The entire network structure consists of ITPNet, TQSA module, PIA module and *prediction head*. TQSA and PIA take the output of ITPNet as an input and perform scene encoding and interaction encoding for trajectory refinement.

B. Additional Qualitative Examples

We visualize additional qualitative examples obtained in diverse interaction scenes. The examples were selected from *Argoverse validation set*. We compare the trajectory samples produced by ITPNet and TRNet to demonstrate the effectiveness of our refinement framework.

B.1. Speed Control Scenarios

In Fig. 5, we present the figures in two columns, where the left figures show the initial trajectory proposals (blue line) and the right figures show both the ground truth (pink line) and the corresponding refined trajectories from TRNet (green line). We consider the scenarios where the target agents slow down or accelerate while interacting with other neighboring agent. In these examples, TRNet generates improved predictions that keep a reasonable distance from the other agent.

B.2. Overtaking Scenarios

Fig. 6 shows three cases in which target agents change lanes to overtake another agents. In all cases, TRNet produces the trajectory predictions that are closer to the ground truth than ITPNet. This demonstrates that our refinement framework effectively utilizes the scene and interaction context by leveraging prior information provided by ITPNet.

B.3. Intersection Scenarios

Fig. 7 shows the scenarios where target agents interact with neighboring agents at intersections. For simplicity, we show only the trajectory of a single neighboring agent most likely to interact with. We see that TRNet produces more reasonable and plausible trajectory outputs than ITPNet. In the case when initial trajectory proposals for two neighboring agents collide, the trajectories of the target agent are refined so that they do not collide with other trajectories.

C. Multi-modal Trajectory Behavior

Fig. 8 shows the multi-modal trajectory samples generated by ITPNet and TRNet. We find that some of the tra-

jectories from ITPNet do not look plausible since they go out of the road boundaries. In contrast, TRNet predicts the trajectories that better fit the scene structures without compromising the diversity of trajectory modes.

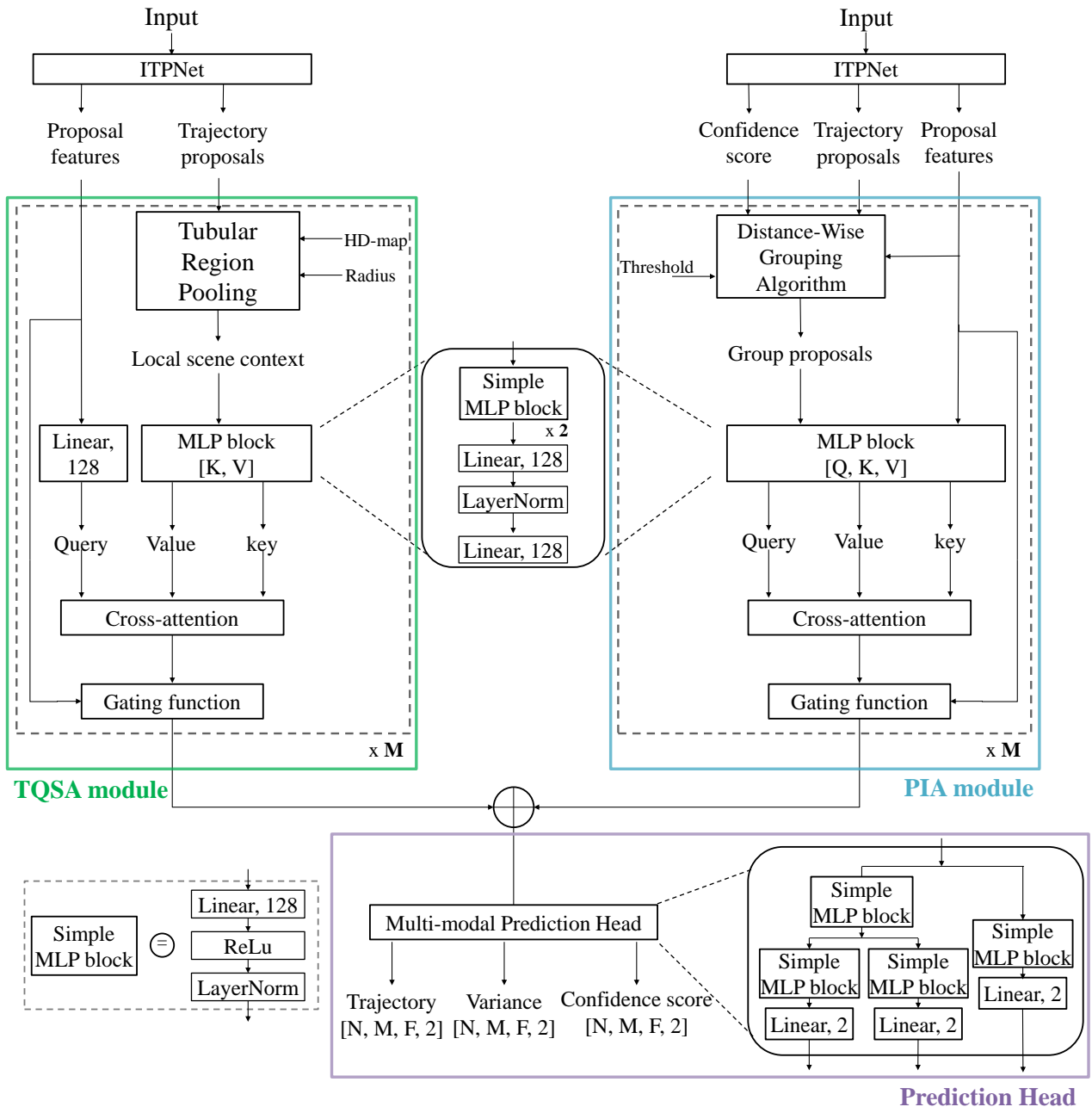


Figure 4. Detailed architecture of R-Pred model.

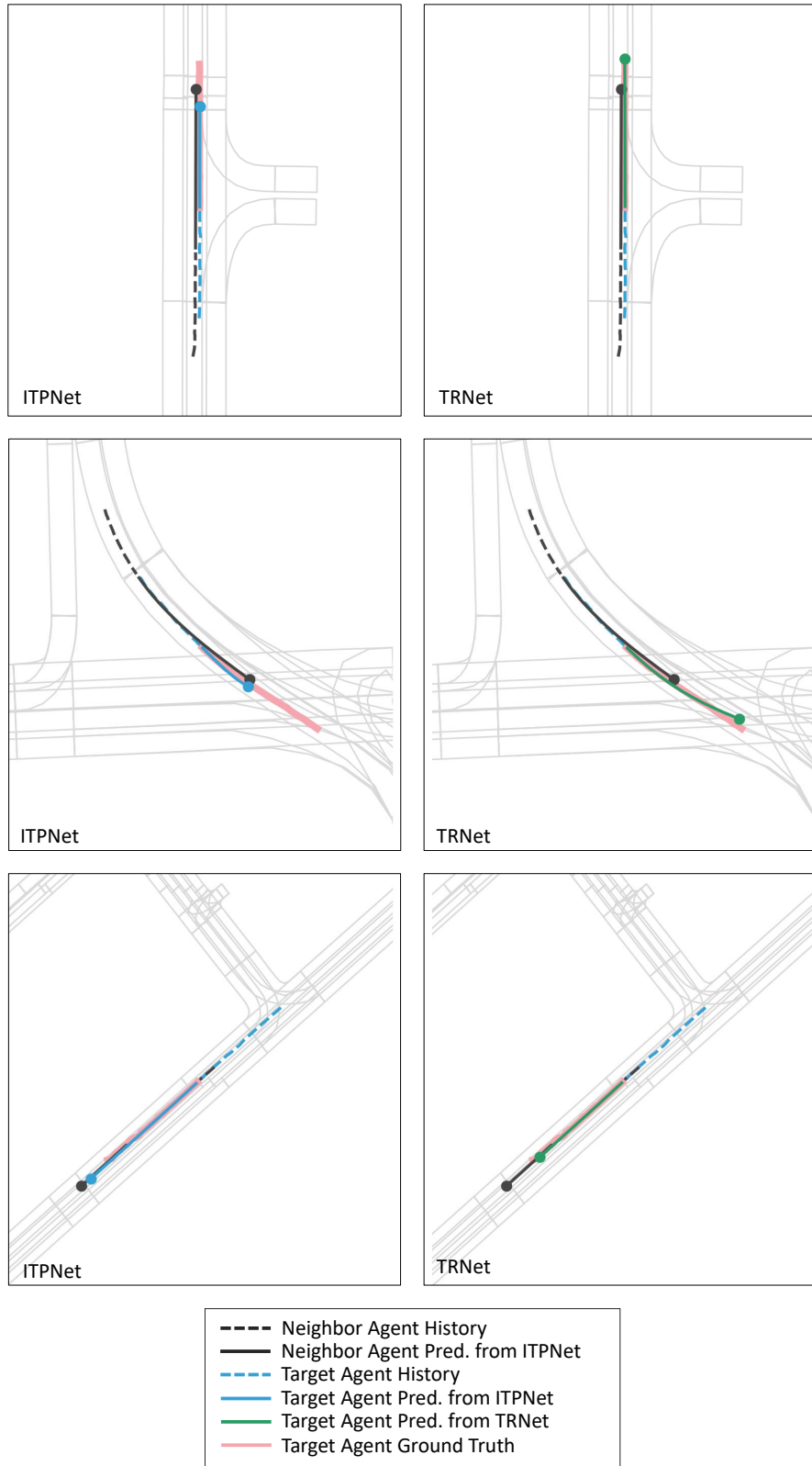


Figure 5. **Visualization of trajectories for several speed control scenarios.** In these scenarios, the target agents slow down or accelerate while interacting with other agents. The proposed refinement framework generates the predictions improved over the initial proposals from ITPNet.

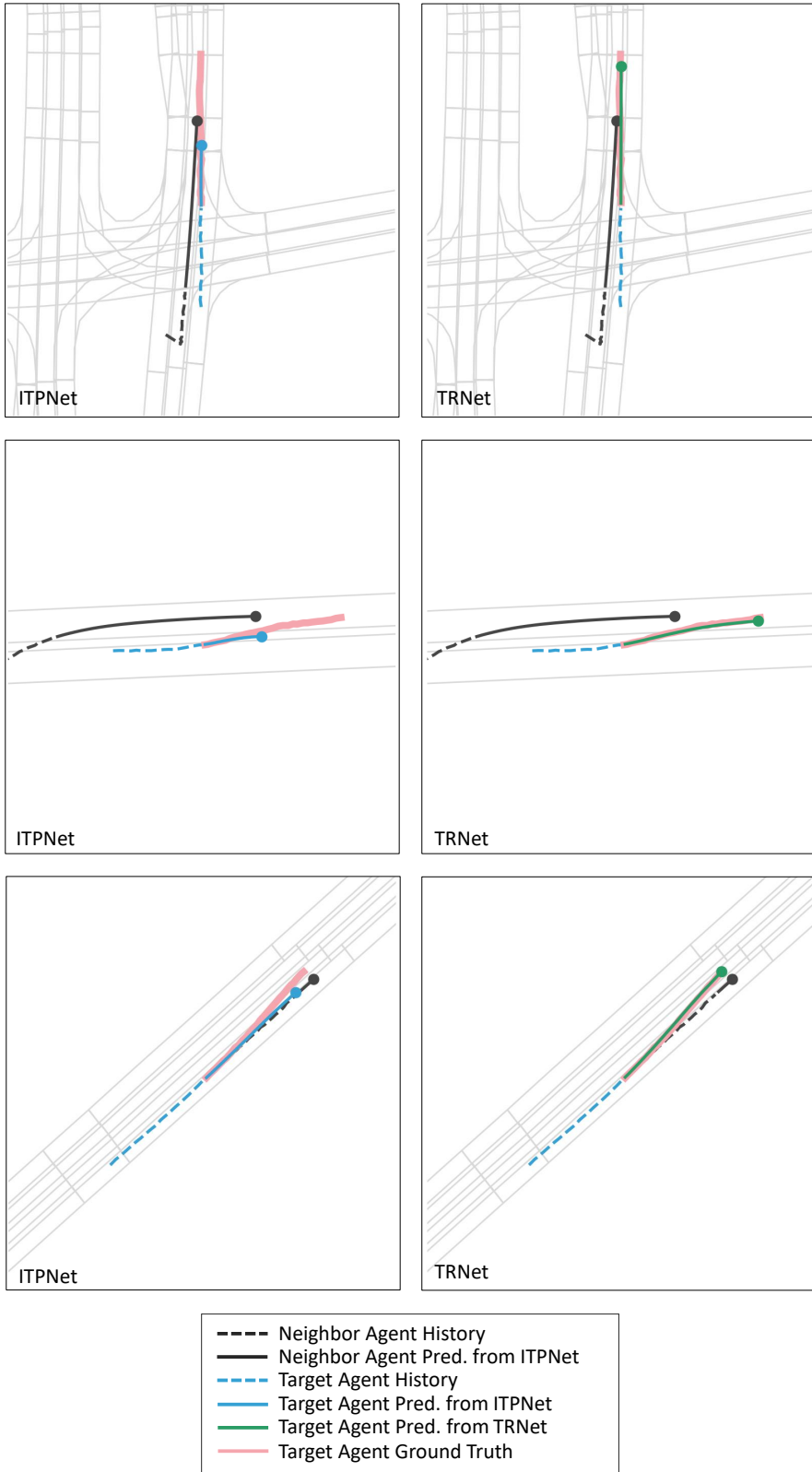


Figure 6. Visualization of trajectories for several overtaking scenarios. In these scenarios, the target agents change lanes to overtake other agents. Considering proposal-level interactions between the agents, TRNet produces trajectory predictions that are closer to the ground truth than ITPNet. Note that conflicts between the initial proposals from two neighboring agents are resolved by the proposed refinement framework.

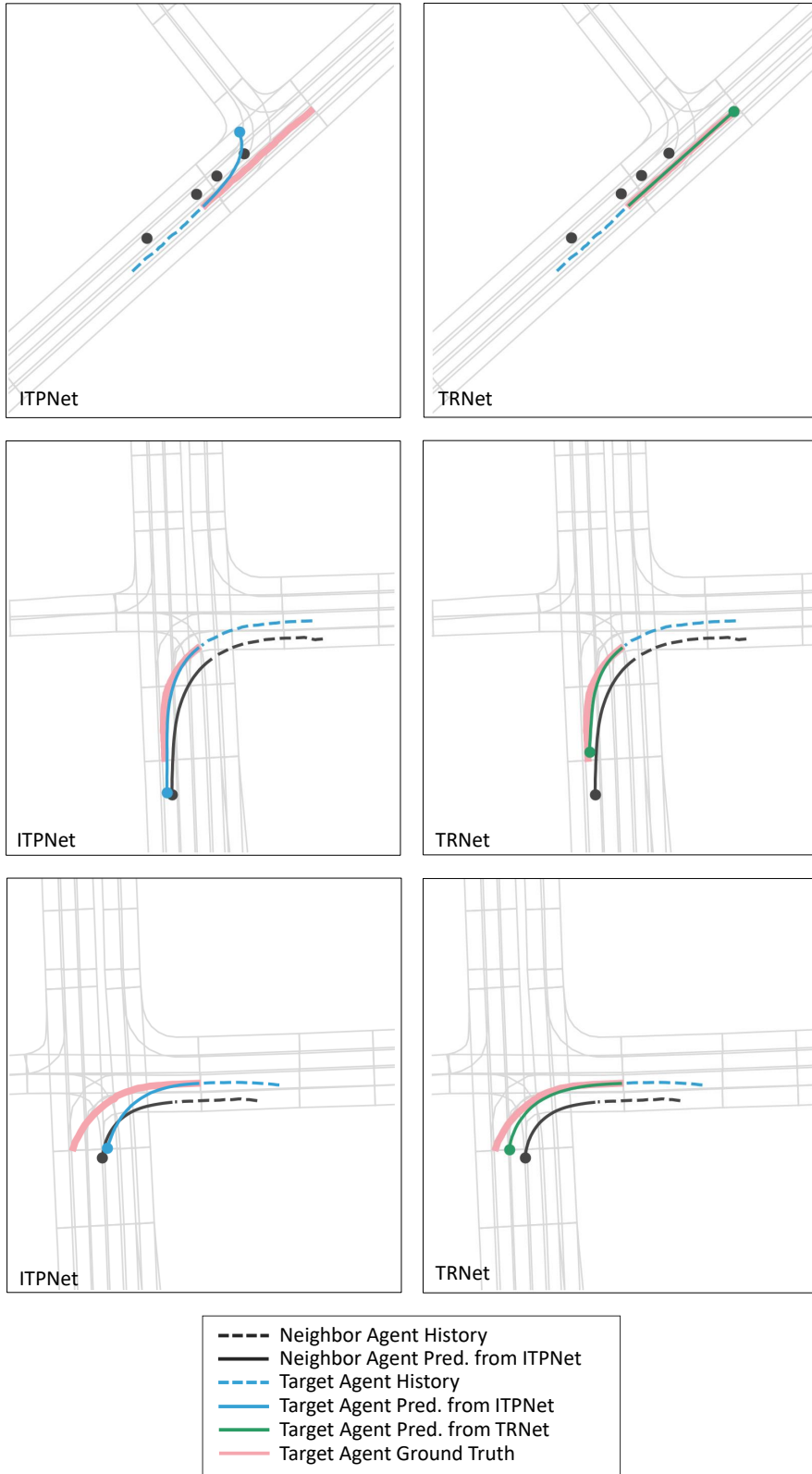


Figure 7. **Visualization of trajectories for several intersection scenarios.** The target agents interact with other agents at intersections. For all cases considered, TRNet produces trajectories that do not collide with other trajectories.

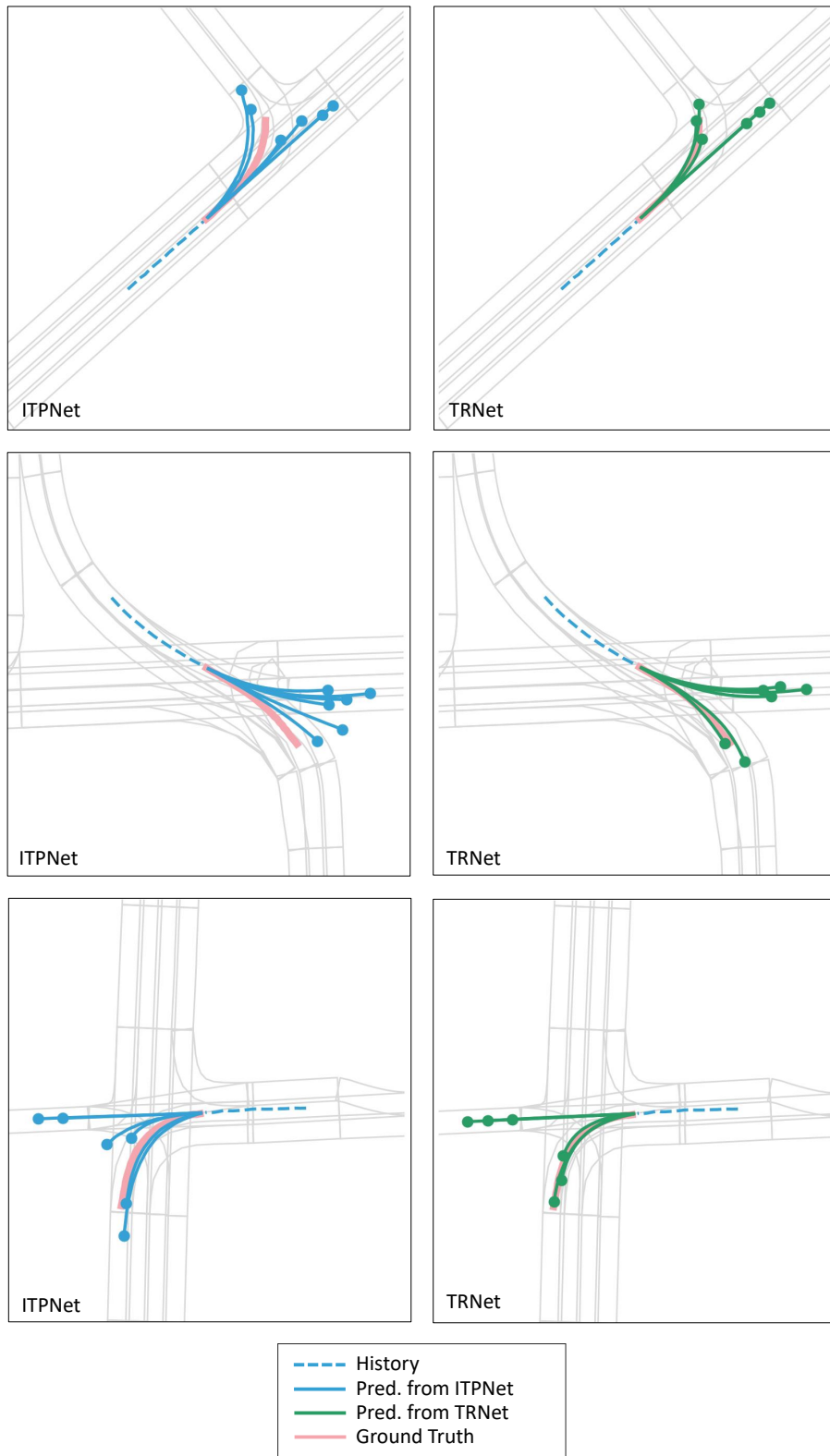


Figure 8. **Visualization of multi-modal trajectories obtained by ITPNet and TRNet.** The multi-modal trajectories predicted by TRNet mostly conform to the scene structures, whereas a few trajectories generated by ITPNet are not physically plausible.